Semi-empirical approach for calibration of CR 39 detectors in diffusion chambers for radon measurements

Patrizia Pereyra Anaya.[1], María Elena López Herrera[1], Daniel Palacios Fernandez[2], Pedro Valdivia[3] and Laszlo Sajo-Bohus[2]

[1]*Pontificia Universidad Católica del Perú*
Av. Universitaria 1801 Lima 32
Lima, Perú.
Buzón-e: pperevr@pucp.edu.pe, mlopez@pucp.edu.pe)

[2]*University Simon Bolivar, Nuclear Physics Laboratory*
Caracas, Venezuela
Buzón-e: lsajo@usb.ve

[3]*Universidad Nacional de Ingeniería*
Lima, Perú
Buzón-e: pvaldivia58@gmail.com

Abstract

Simulated and measured calibration of PADC detectors is given for cylindrical diffusion chambers employed in environmental radon measurements. The method is based on determining the minimum alpha energy (E_{min}), average critical angle ($<\theta_c>$), and fraction of ^{218}Po atoms; the volume of the chamber (f_1), are compared to commercially available devices. Radon concentration for exposed detectors is obtained from induced track densities and the well-established calibration coefficient for NRPB monitor. Calibration coefficient of a PADC detector in a cylindrical diffusion chamber of any size is determined under the same chemical etching conditions and track analysis methodology. In this study the results of numerical examples and comparisons between experimental calibration coefficients and simulation purpose made code. Results show that the developed method is applicable when uncertainties of 10% are acceptable.

Keywords: Radon; PADC; calibration factor; Monte Carlo simulation.

1.- INTRODUCTION

Approximately half of the human exposure to radiation is due to indoor airborne radon gas (^{222}Rn) and his short-lived progeny. Polyallydiglicolcarbonate (PADC) type nuclear track detectors (NTDs) are conveniently employed for integral measurements of environmental radon gas. The average airborne radon concentration can be converted into the radon decay product concentration when the equilibrium factor is either monitored or known to have a given value [Dixon 1999]. Thus, the induced track density is converted into a dose of radon decay products.

The use of PADCs with diffusion chambers is the most reliable nuclear track methodology to determine time integrated radon concentration levels; most conveniently applied for large scale survey under different environmental conditions. The methodology requires detectors to be calibrated in purpose made radon chambers with a relatively high concentrations (400-800 Bq.m^{-3}).

Concerning indoor and workplace radioprotection aspects related to radon many worldwide emerging laboratories are engaged in radon measurements employing nuclear track methodology; that has several advantages as reported elsewhere. However, most of the laboratories among the developing countries lack of financial support to acquire commercial radon monitors, as well as radon chambers or open ^{226}Ra sources.

That consequently requires some alternative procedure to determined calibration of purpose made diffusion chambers. One of them is the Monte Carlo simulation. The drawback of Monte Carlo calculations is the sensitivity of the computed values for various input data which sometimes are not accurately known. Nevertheless, the validity of the calibration factor by simulation has to be validated by experiment.

1.1. Theoretical aspects on calibration

Radon concentration measurements can be performed employing e.g. PADC (CR-39^{TM}) and a diffusion chamber closed at the top with a semi-permeable filter; in this case the detecting device is positioned in such a way that only the ^{222}Rn gas diffuses into the chamber while the radon progeny, dust and water vapor are stopped by the thin film. A schematic sketch of a cylindrical diffusion chamber is given in Figure 1. In that the geometrical parameters are shown: H chamber height, R the cylinder base radius and R_{det} PADC detector radius.

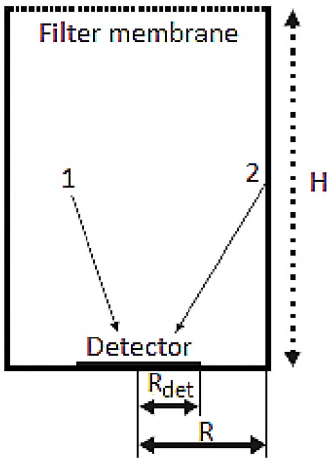

Figure1. A cylindrical diffusion chamber (with a height H and base radius R) with PADC detector (with radius R_{det}) placed on the inner bottom.

As the radon atoms randomly move inside the chamber at any point a given probability exists to experiment alpha decay creating its progeny; that in turns with a restricted random walk (deposition on the chamber wall) experiments a transformation in volume of the chamber. Physical processes to be considered are: the alpha emitters in air (^{222}Rn, non-deposited fraction of ^{218}Po and ^{214}Po) denoted by "1" in Figure 1, and those fraction of ^{218}Po and ^{214}Po that are deposited on the chamber wall, denoted by "2" in the same figure.

The total sensitivity S_{sim} of the detector [track/m^2/(Bq.s.m^{-3})] is the sum of the partial sensitivities that are multiplied by factors representing the partitioning of radon progeny between air and the chamber wall and can be calculated as:

$$S_{sim} = \rho_0 + f_1\,\rho_{1a} + \left(\frac{V}{A}\right)\left[(1-f_1)\rho_{1w} + \rho_{4w}\right] + \rho_{1p} + \rho_{4p} \qquad (1)$$

Where:

ρ_0, ρ_{1a}, ρ_{1w} and ρ_{4w}: sensitivity respectively to ^{222}Rn ^{218}Po, ^{218}Po and ^{214}Po in chamber air volume and wall ρ_{1p} and ρ_{4p}: sensitivity respectively to ^{218}Po and ^{214}Po deposited on the detector.

It is reasonable to assume that all ^{214}Po-atoms are deposited before decay i.e. $f_4 = 0$ justified by its relatively large half- life, while f_1 can vary between 0 and 1. All the variables in Eq. (1) are determined by Monte Carlo simulations.

The average radon concentration C is calculated by, $C = k\,\rho$, where k is the calibration coefficient ($k=1/S$) and ρ is the track density per unit irradiation time (track/m^{2}s).

One of the typical ways to apply the Monte Carlo simulations to study the detector response in diffusion chambers, requires the knowledge of the minimum impinging alpha energy (E_{min}) and the energy dependence of the critical angle $\theta_c = f(E)$, or the mean critical angle $\langle\theta_{crit}\rangle$, and the air fraction of ^{218}Po (f_1). These parameters depend on the chemical etching conditions, the diffusion chamber geometry and the track analysis method.

The sensitivities of the CR-39 device also depend on detector size, manufacturing and , and chamber dimensions. Having determined experimentally values of minimum energy and dependence of the critical angle with energy for a given etching conditions, Monte Carlo simulations provide the calibration factor for any chamber geometry and detector dimensions.

2.- MATERIALS AND METHODS

2.1. Considerations for Monte Carlo simulation

2.1.1. Range of variation of the mean critical angle

The critical angle θc is the minimum angle at which alpha-particles will induce a latent a track in the detector. In our case conveniently proved adequate for this study the TASL type CR-39 SSNTD, with average value of θ_c=15° (measured with respect to the plane of the detector). This value was found to be suitable for particles registration [Hafez et al., Naim, 1992; Misdaq et al., 2001], assuming that a layer of about 10 µm is removed during etching from the surface of the detector. Askari et al., [2008] reported different critical angles for various radionuclides i.e. 44.7° for ^{222}Rn, 39.8° for 218Po, and 21.7° for ^{214}Po. Mansy et al. (2006) argued that although the critical angle is energy dependent, varying from 10° to 30°, as a suitable approximation the mean value of the critical angle can be taken for sensitivity calculation of the detector. Etching conditions affect the bulk etching rate and the critical angle [Somogyi 1980; Misdaq et al., 2001; Abu-Jarad et al. 1980].

The theoretical critical angle of the CR-39 detector is determined by the equation [Nikezic et al., 2002]:

$$\theta_c = sin^{-1}\left(\frac{1}{V_0}\right) \tag{2}$$

where V_0 is the maximal value of the V function (=Vt/Vb). They adopted the V function given by Durrani et al., [1987] and found a theoretical critical angle of 7.63°.

The average value of the critical angle is given by:

$$\theta_c = \frac{1}{\Delta E}\int_{E_{min}}^{E_\alpha} \theta_{c_i}(E_{\alpha_i}^{res})\, dE_{\alpha_i}^{res} \tag{3}$$

where $\Delta E = E_{\alpha} - E_{min}$, $\theta_c(E_{\alpha i}^{res})$ represent the analytical equations of the critical angles θ_c as a function of the alpha-particle residual energy $E_{\alpha i}^{res}$. A mean critical angle approximately equal to 20° was found by Durrani et al., [1987].

Using PADC detectors in can and bare modes, Abo-Elmagd et al., [2009] estimated the equilibrium factor F between radon and its daughters. They used an equation that is valid for a critical angle equal to 20° for diffusion chambers satisfying the following conditions: radius $r \leq 3.5$ cm, height $h \leq 10$ cm, and $0.4 \text{ cm} \leq V/A \leq 1.3$ cm.

Considering the critical angles values reported by different authors, in this paper we assume the average critical angle ranging from 5 ° to 45° depending on experimental conditions. Patiris et al., suggested that deposited radon daughters on PADC detectors could undergo discriminative detection of using simulation.

2.1.2. On the minimum energy of alpha particles

The detector has a wide energy window for α-particles registration (from threshold value of $E_{\alpha,th}$=200keV up to 40 MeV) [Askari et al., 2008; Durrani et al., 1987; Saeed 2014]. There is not minimum distance from the detector to induce an etchable track [Abu-Jarad et al., 1980], since all alpha particles emitted by radon daughters deposited onto detector surface are registered. Therefore, for the purpose of recording alpha particles emitted from radon or its progeny, PADC detectors effectively do not show an upper energy value.

According to Khayrat et al., [1999], tracks formed by alpha particles with energies as small as 100 keV can be visualized applying small etching times. With limited applicability since in that region of values no linear response dominates. Fromm et al., [1988] and Reza et al., [2013] did suggested $E_{\alpha,th}$ 0.5 MeV for CR-39 detectors etched in 6 N NaOH at 70°C for 2h.

According to the literature, in the simulations we consider that the minimum energy is in the range of 0.1 to 0.5 MeV depending on the device response linearity.

2.1.3. Fraction of ^{218}Po atoms decaying in the diffusion chamber active volume

The air fraction of ^{218}Po has its importance in sensitivity determination by Monte Carlo simulations as given by Nikezic et al., [2014]. The value depends on the diffusion coefficient of ^{218}Po atoms in air. Thus, the concentration of aerosol particles in the chamber volume influences the system dynamical response. That in principle, may also depend on the relative humidity, presence of electrostatic field within the chamber and the chamber matter itself [Koo et al. 2002 and 2003], these authors conducted experiments to quantify the influencing factors reporting that the best f- value for the non-deposited fraction was 0.4 for all cases. They concluded that the deposition fraction does not depend on the shape and dimensions of the diffusion chambers, nor on the internal surface matter.

McLaughlin et al., [1994] did show that a total deposition of ^{218}Po exists, however according to Pressyanov [2008], the volume fraction of ^{218}Po (f_1) can vary within 4–40% over the studied range of diffusion coefficients, while ^{214}Bi ($+^{214}$Po) atoms are practically entirely deposited. Results obtained by Nikezic et al., [2014], indicate that 6.6% of ^{218}Po atoms decay in the chamber volume and the remaining 93.4% decay from the deposited state on the inner walls of the chamber.

The deposition fractions determined by different authors were very different. The large discrepancies among different approaches in the determination of the deposition fraction of ^{218}Po underlined the necessity for additional experimental and theoretical work on this problem. In addition, there is a problem that has been theoretically demonstrated by Palacios et al. [2005] and Nikezic et al., op.cit that in fact exists a non-uniform deposit of radon progeny inside chamber wall. Taking account the results described above, in this paper we consider values ranging from $0 < f_1 < 0.4$.

2.1.4. Influence of different material in diffusion chambers

According to Pressyanov et al. [1999] there is a significant difference between the sensitivity of metal-made and plastic cylindrical diffusion chambers. They found that experimental sensitivity for metal-made chambers is in good agreement with the theoretical model based

on diffusion of radon progeny inside the chambers. In which uncertainty in the sensitivity might be related to possible variations of the diffusion coefficient of ^{218}Po atoms. This uncertainty (for chambers of d=8 cm and h=7.5 cm) is expected to be less than 10%. For plastic chambers of the same size they found a difference of 15% from the predicted by the diffusion model. They concluded that the deposition of ^{218}Po atoms in plastic chambers cannot be explained only by a simple diffusion. In correspondence with the above, values and ranges of the parameters used in MC simulations in this paper were: E_{min} from 0.1 MeV to 0.4 MeV, mean critical angle from 5° to 45° and f_1 up to 0.4.

2.2. Experimental part

The National Radiation Protection Board or NRPB, developed a device for personal radon dosimetry in mines; in that PADC detector (known by its trade name CR-39^{TM}) is enclosed in a plastic holder made of an upper and lower cover which snaps together, has proved to be the most interesting device, especially because of its highly consistent response even for different chemical etching conditions and different etching reagents. This device reported in Figure 2 illustrates a passive radon monitor, which consists of a track detector placed inside a container having a cm height, where radon can diffuse, thus referred to as a diffusion chamber.

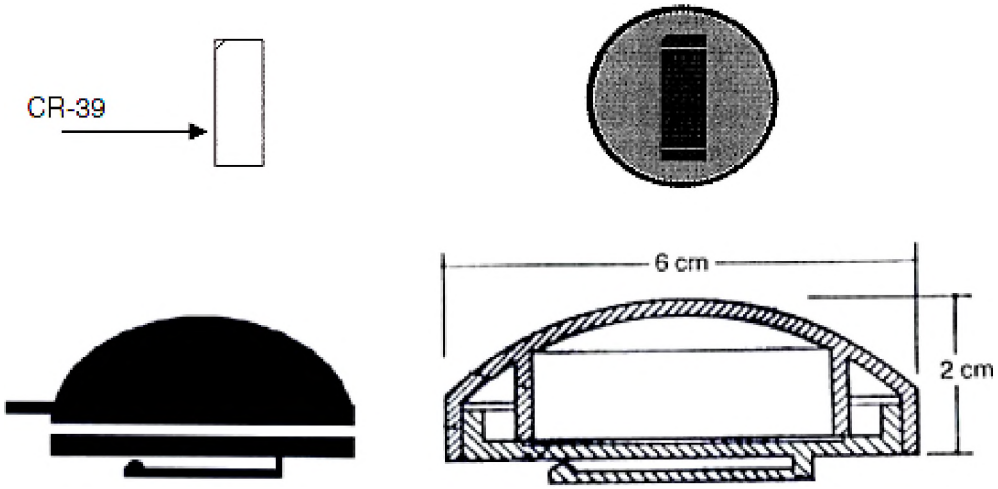

Figure 2. Schematics of a NRPB type of radon detector that shows geometrical parameters and passive detector

The two covers one flat and the other having a spherical sector fit tightly to exclude moisture, dust or radon progeny. The diffusion time of radon into the detector housing is long enough to exclude the ingress of ^{220}Rn (thoron). This type of passive radon monitor have been tested also in a severe environmental conditions as those found in mines and satisfactory results have been always achieved as tests in several inter-comparison exercises proved. Table 1 shows the different etching conditions of CR-39 detectors from different providers and the used calibration factors. The NRPB-device copes well with the following requirements [Mamont-Cieśla et al. 2010 Howarth et al 2003, 2007, 2006]:

- High sensitivity, negligible fading, compactness, ruggedness, relatively low cost;
- Response nearly independent of environmental conditions (including high humidity, altitude pressure, presence of mud, etc.).

Table 1. Etching conditions and calibration factors for CR-39 detectors, from different providers, exposed in NRPB diffusion chambers

Chemical etching conditions			**Sensitivity**
Concentration of NaOH (%)	Temperature (°C)	Duration (h)	($tr.cm^{-2}$ /$kBq.h.m^{-3}$)
22	80	18	2,5
20	81	18	2,7
20	81	18	2,5
20	40	11,5	2
20	80	18	2,6
20	80	18	3,4
25	75	8	2,8

Due to its reliability, this monitor was employed as reference to calculate the average radon concentration at the selected site. Several types of diffusion chambers of different sizes were exposed at a radon environment together with the NRPB monitor. All monitors were

exposed at the same place and environmental conditions (average humidity 90% and average temperature 16°C) during the same period of time (2 months). After exposure the CR-39 detectors were etched in a 6N NaOH solution at 70° for 6 hours. According to Table 1, the etching conditions closest to the used in our experiment are 25% NaOH at 75°C during 8 hours. Thus, the sensitivity used to calculate the radon concentration from the induced track densities in the PADC of NRPB monitor was 2.8 (tr.cm^{-2}) / (kBq.h.m^{-3}). A light transmission microscope with magnification of X20 was used for the automatic track counting using a digitalized image analyzer. For each detector on average 100 fields of view were analyzed. The reference chambers were used to determine E_{min}, $\langle\theta c\rangle$, and f_1 by means of a self-developed program based on Monte Carlo simulations. Table 2 shows the geometric parameters of the studied diffusion chambers.

Table 2. Characteristics and geometry values of diffusion chambers

Chamber Code	**Material and geometry**	**Diameter (cm)**	**Height (cm)**	**Volume (cm^3)**
A	Metal cylinder	8,3	3,3	258
H	Plastic cylinder	6,0	7,0	200
F	Plastic cylinder	6,8	9,0	470
E	Metal cylinder	7,2	9,8	400
N	Plastic cylinder	5,4	2,0	34
I	Plastic truncated cone	D_{major}=6,5, D_{minor}=3,8	7,3	160

Chamber Code	Material and geometry	Detector radius (cm)	Chamber diameter (cm)	Chamber height (cm)	Sensitivity
A	Metal cylinder	0,27	4,15	3,3	0,62
F	Plastic cylinder	0,27	3,40	9,0	0,51
E	Metal cylinder	0,29	3,60	9,8	3,21
N	Plastic cylinder	0,27	2,70	2,0	0,30
I	Plastic truncated cone	0,29	2,58	7,3	0,36

2.2.1. Description of the purpose made Monte Carlo program

The partial sensitivities of a CR-39 detector to radon and its progeny were calculated by a self-developed computer program based on Monte Carlo simulations. The program performs simulations of alpha particles (randomly sampled) emitted from the volume and inner surface of the chamber and their registration by the detector.

For calculations of partial sensitivities of the CR-39 detector to ^{222}Rn, ^{214}Po and ^{218}Po three parameter were considered: the mean critical angle $<\theta_{crit}>$ and minimum energy (E_{min}) of the incident alpha particles, and airborne fraction of ^{218}Po atoms (f_1). Threshold energy (E_{min}) and the mean critical angle are determined from the experimental sensitivities, obtained in the different diffusion chambers exposed to the same radon concentration C_{Rn} as:

$$S_{exp,i} = \frac{\dot{\rho}_i}{C_{Rn}}, \tag{4}$$

where ρ_i is the net track density rate registered in each detector (background corrected).
The values of partial sensitivities and fraction f_1 that generate the least square deviations between the simulated and the experimental total sensitivities, or Min $(S_{exp,i} - S_{sim})^2$, enables the estimation of the corresponding ΔE and $<\theta_{crit}>$.

The program starts with reading the initial alpha-particle energies (^{222}Rn 5.49 MeV, ^{218}Po 6.00 MeV, ^{214}Po 7.68 MeV), experimental total sensitivity ($S_{exp,i}$), energy threshold (E_{min}), average critical angle $<\theta_{crit}>$, airborne fraction of ^{218}Po atoms (f_1), radius and height of the diffusion chamber (r, h), and detector radius (r_{det}).

The next step is to determine the coordinates of the emission points of the volume in front of detector from which the alpha particles have non-zero detection probabilities, i.e., the so called “effective volume”. For the calculation of partial sensitivities only the initial points of alpha particles within the effective volume are sampled. The effective volume defines the minimal and maximal distances in air from which the emitted alpha particles can be detected; an alpha particle cannot be detected if is emitted outside this volume.

2.2.1.1. Subroutine to simulate the effective volumes

This program calculates the effective volume in front of the CR-39 detector for alpha particles of a given energy. The whole space in front of the detector is examined by the selection of random points in the volume of the diffusion chamber. Reduction of the alpha particle energy from the emission point to the detector caused by air was calculated using the SRIM 2013 software and the corresponding energy-distance dependences.

Only those points which fall within the effective volume are taken as starting points of the alpha particles for the calculation of partial sensitivities. The effective volume, or its fraction in the diffusion chamber, is calculated by applying the rejection technique.

2.2.1.2. Calculation of detector sensitivity

Three different sources contribute to the total track density (and sensitivity): (a) radon and progeny in the chamber air (volume fraction), (b) progeny deposited on the inner chamber wall including the filter opposite to the detector (wall fraction), and (c) progeny deposited on the detector itself (plate out). Three separate subroutines were prepared, one for each source. The incident alpha particle energy (i.e., isotopes) is defined in the program, which automatically changes them. To ensure 0.1% of the relative standard error the number of "registered alpha particles" was taken as 10^5.

To calculate the detector sensitivity, input data about the chamber (radius and height) and detector (radius) dimensions are needed. It is assumed that the detector has a circular shape, whose area is the same as that of the detector used in the experiments. Several subroutines are included in the MC code such as for the:

a) volume fraction: it calculates the sensitivity of CR-39 that is located in the bottom of a cylindrical diffusion chamber, assuming that alpha emitters are in the chamber volume. The program calculates partial sensitivities of the CR-39 detector in a given diffusion chamber to ^{222}Rn and ^{218}Po. The output results are given in cm.

b) wall fraction: it calculates partial sensitivities of the detector to ^{218}Po and ^{214}Po deposited onto the inner chamber wall. The output results of partial sensitivities are also given in the cm. It is assumed that radon progeny are uniformly deposited on the inner chamber wall.

c) top fraction: it calculates partial sensitivities of the detector to ^{218}Po and ^{214}Po deposited onto the top chamber (inner part of the semipermeable membrane). The output results of partial sensitivities are also given in the cm. It is assumed that radon progeny are uniformly deposited.

d) plate out: it calculates the sensitivity to radon progeny (^{218}Po and ^{214}Po) deposited onto detector (plate out). The calculation algorithm is similar to that used in the subroutine for the wall fraction, but in this case it is not necessary to determine the effective surface area since it is precisely the detector surface. It was assumed that progeny are deposited homogeneously onto the detector itself. The results are also given in cm.

Flow-diagram of cycles given in Figure 3 estimate the energy threshold, average critical angle and fraction f_1 that generates least squared deviation between simulated and experimental total sensitivities.

The parameters found are those that characterized the formation of registered tracks in CR-39 detectors for the used etching conditions and mode of track analysis (E_{min} and $<\theta_{crit}>$), as well as the behavior of ^{218}Po atoms inside the chamber (f_1).

The above-described process was repeated with a smaller step around the values that conditioned the minimum found. During the successive approximations the $(S_{exp}-S_{teor})^2$ function showed an oscillatory character, presenting local minima, but in all cases converged to an absolute minimum corresponding to the desired solution.

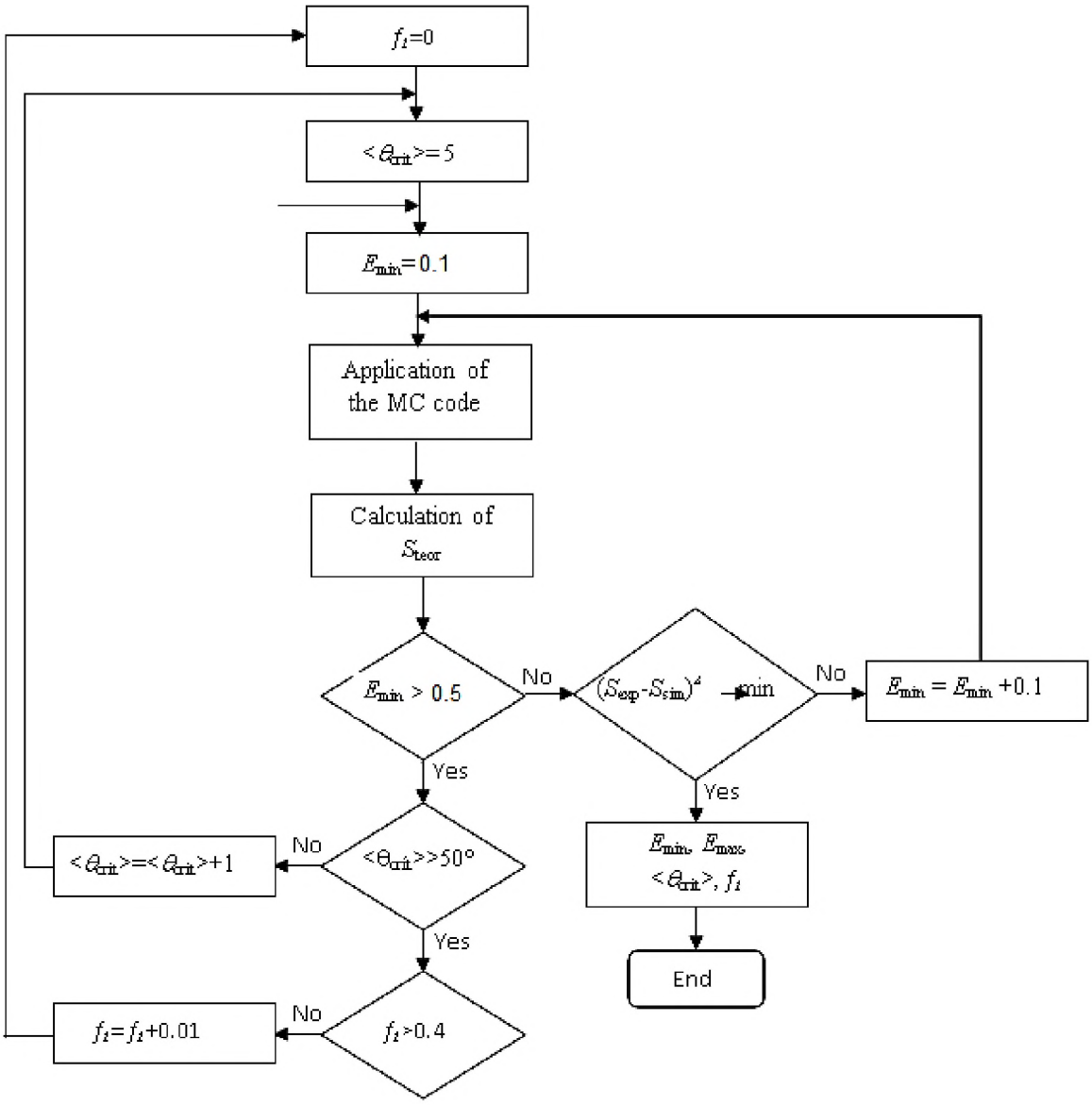

Figure 3. Flowchart of cycles used to estimate the energy thresholds, average critical angle and the f_1 fraction.

3.- RESULTS

Figure 4 illustrates a numerical example of convergence of the successive approximations. In this case, the expected value of the mean critical angle was 20°. The different points corresponding to the same critical angle are related to assigned values of E_{min} and f_1 in the cicles. As can be seen in Figure 5, the sum of square deviations, considering all possible combinations of E_{min} and f_1 for each critical angle value, also converge for $<\theta_c>=20°$.

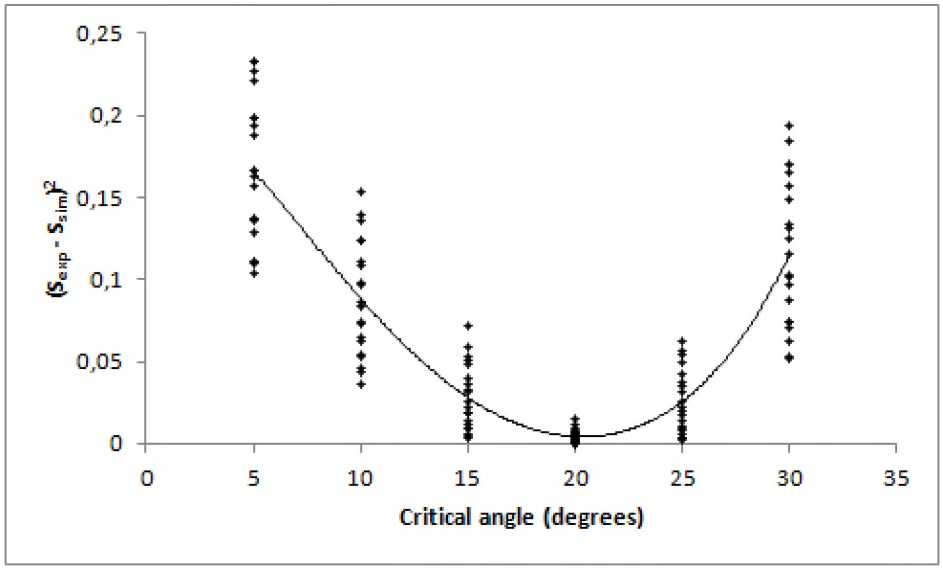

Figure 4. Numerical example of convergence of the successive approximations

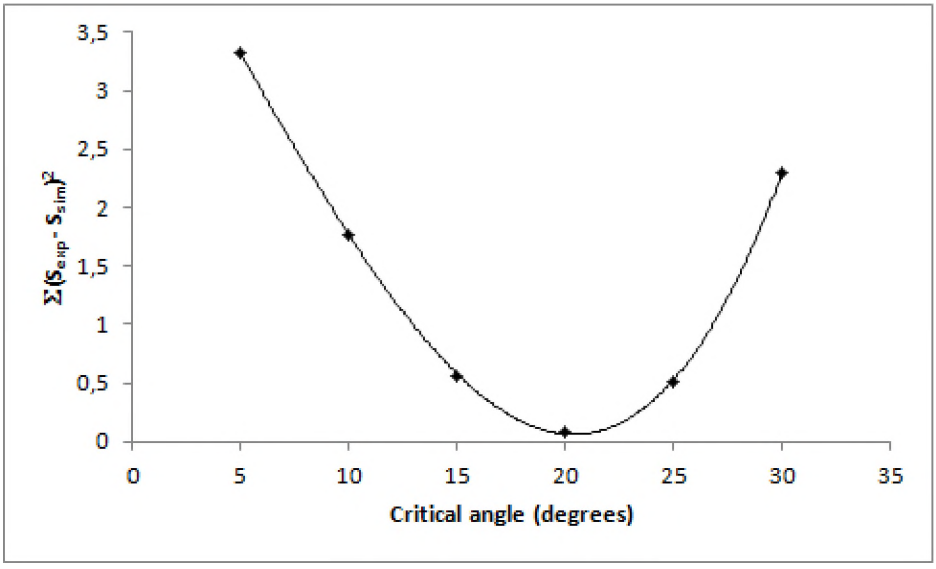

Figure 5. Numerical example of convergence: $<\theta_c>=20°$.

In the same way, the Monte Carlo simulations results for the other diffusion chamber are shown in the Figure 6.

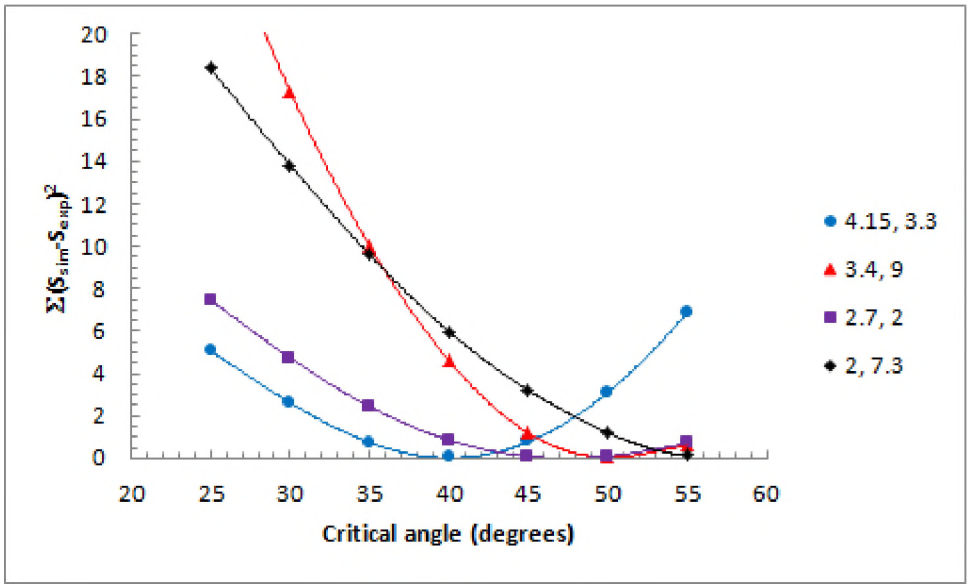

Figure 6. Numerical example of unit square deviations for different chambers.

Introducing in the simulation sensitivity values obtained experimentally (S_{EXP}), together with the geometric parameters of each chamber and detector, through successive approximations E_{min}, $\langle\theta c\rangle$ and f_1 values were determined. The latter generate the least squared deviation between S_{EXP} and the calculated sensitivity (S_{cal}). In the following table these values are presented together with the minimum values of the deviations between S_{EXP} and S_{cal}.

Because very low values of sensitivities in the different chambers were obtained, it was considered that the radon concentration inside the different diffusion chambers was approximately 50% of that obtained in the NRPB monitor, justified by the use of a relatively low permeability membrane to radon, the presence of water vapor condensation on the membrane and on on a lower degree on the detector itself due to the environment relative high humidity, deposition of suspended dust particles and other limiting factors. Applying the reduction factor our results compare well with those reported in the literature.

Given that the physically E_{min} and the critical angle should be independent of the chamber and detector geometry and dimensions and detector, their mean values were estimated. Average values, the test chamber and detectors, the corresponding sensitivities were determined. With the values of sensitivities of each detector exposed track densities provided radon concentrations in the study site. The Table 6 shows the estimated radon concentrations and percentage deviations (Calculated as (|Exp.-Theo.|/|Exp.|)X100) compared to that obtained with the NRPB monitor.

Table 6. Experimental results and compared with calculated values.

Monitor	E_{min} (MeV)	$\langle\theta_c\rangle$ (degrees)	f_1	S_{exp} (cm^{-1})	S_{cal} (cm^{-1})	Min
F – b	0,2	40	0,2	1,24	1,23	3,05E-05
A – b	0,3	50	0,0	1,03	1,02	5,77E-05
N-b	0,1	45	0,0	0,60	0,64	1,39E-03
I – a	0,1	55	0,0	0,72	0,75	2,24E-03

From the above Table values, the parameters E_{min}, $\langle\theta_c\rangle$ y f1 for the four test-cameras are 0,175 MeV, 47,5 ° and 0,05, respectively.

To assess whether the use of these parameters reproduced radon concentration estimated with the NRPB monitor, these were used in the main program MC to determine partial and total sensibilities for each of the camera. In the following table the results of the sensitivities and calibration coefficients are reported; these data provide radon concentrations estimated for each diffusion chamber employing track densities.

Also, provide percentages deviations from the value given by the NRPB device (97,25 Bq.m-3); uncertainties in measurements of radon concentration do not exceed 30%.

Table 7. Radon concentrations estimated for each diffusion chamber employing track densities and comparison with NPBR-monitor reference value

Monitorcode	R (cm)	H (cm)	S_{NRPB}	S_{recalc} (cm)	k_{recalc} Bq.s.cm^{-3}/ (tr.cm^{-2})	k_{recalc} Bq.month.m^{-3}/ (tr.cm^{-2})	$C_{Rn\ rec}$ (Bq)	□ (%)
A	4,15	3,30	1,24	0,96	1,04	0,40	125,15	28,7
F	3,40	9,00	1,03	0,92	1,09	0,42	108,52	11,6
N	2,70	2,00	0,60	0,58	1,74	0,67	101,75	4,6
I	2,00	7,30	0,72	0,86	1,16	0,45	80,95	16,8

By means of the developed program, with these parameters we can determine the calibration coefficient of a PADC detector in a cylindrical diffusion chamber of any size, if chemical etching conditions and mode of track analysis are the same as the used for calculations.

The corresponding f_1 fraction is taken according to the A/V ratio of the chamber. In other words, if another type of diffusion chamber is to be used, is not necessary to experimentally determine the calibration coefficient by their exposure to known radon concentration. Instead, simply enter their dimensions and the obtained values of E_{min} and $<\theta_{crit}$ in the developed Monte Carlo code. It is important to emphasize that the etched conditions and track analysis should remain unchanged.

Although the present experimental estimation of the critical angle is in good agreement with Fromm et al. [1988], the use of different etching conditions and acquisition apparatus resulted in a greater critical angle (15° difference) than the angle found by Dörschel et al. [2002].

3.1. Validation of the simulation method

To evaluate the performance of the developed program we use experimental results of sensitivities reported by different authors. Basic information of the chamber and etching conditions are given in Table 3. In experiments, rectangular detectors were used but in

calculation circular detectors were assumed with the same surface area as the used in measurements. Most of the diffusion chambers were conical, so for simulations we used their mean radii.

Table 8. Experimental conditions for comparison experimental and simulated sensitivities.

Chamber number	Reference	Dimensions and shape of the chamber	Estimated detector radius (cm)	Etching conditions
1	Mahlobo et al.,(1992)	Conical chamber Mean radius=3.05 cm Height= 9.5 cm	1,41	6 M NaOH, 70 ◦C, 12 h
2	Garawi (1996)	Conical chamber Mean radius= 3,625 cm Height= 4.7 cm	1	6 M NaOH, 70 ◦C, 2.5 h
3	Antovic et al., (2007)	Conical chamber Mean radius= 2,9 cm Height= 5,3 cm	1,775	6.25 M NaOH, 70 ◦C, 7 h
4	Ismail et al., (2011)	Cylindrical chamber Radius= 3 cm Height= 7 cm	0,69	6 M NaOH, 70 ◦C, 9 h

Comparison between experiments and calculation is given in Figure 7. Black "x" represent results obtained by MC calculations and red points represent experimental values given by Mahlobo et al., [1992], Garawi [1996], Antovic et al., [2007], and Ismail et al. [2011].

Positive values from error bars corresponding to the difference between sensitivity to f_1=1 and the obtained (f_1=0,5), while the negative values corresponding to the difference between the sensitivity obtain to f1=0,5 and the obtained (f_1=0).

The mean critical angle and minimum energy were assumed to be 20° and 0.1 MeV, respectively. These values were taken from literature [Mansy et al., 2006; Khayrat et al., 1999] and it may not correspond to the different etching conditions and characteristics of the diffusion chambers. Since the detector sensitivity (f_1) depends on volumetric fraction of

^{218}Po, three calculations were performed assuming f = 1, 0.5, and 0. Calculation results are presented as scattered points with the uncertainty bar. The upper value of the bar is obtained for f = 1, while the lower is for f = 0. Scattered points correspond to f_1 = 0.5.

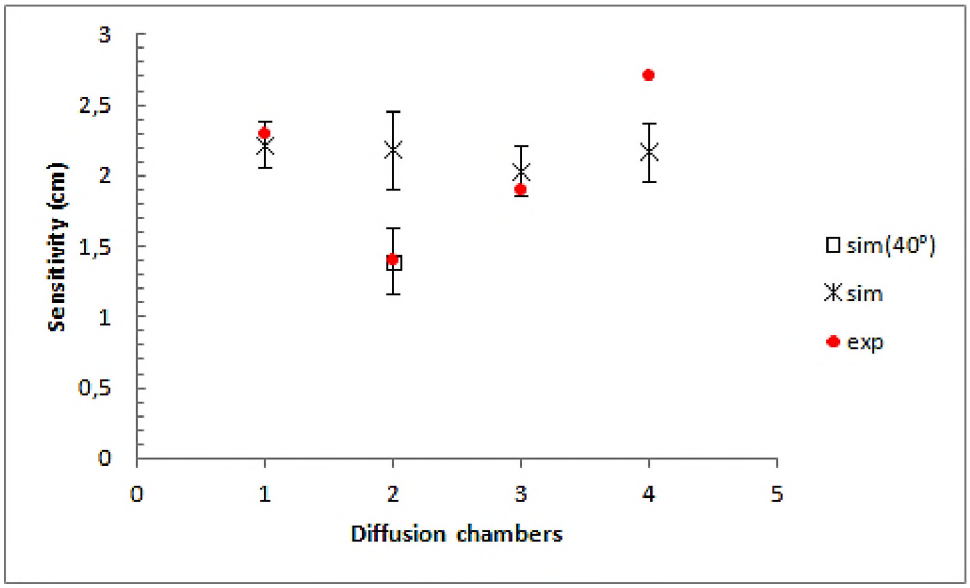

Figure 7. Comparison of experimental and simulated sensitivities for different chambers, detector radii, and etching conditions

Inspection of Figure 7 shows that the result given by Ismail et al. [2011] is well above the calculated sensitivity. Similar results were obtained also by Nikezic et al., [2014]. The experimental sensitivity for chamber (2) is well below the calculated value. Probably, the short etching time, different bulk etch rate and others influencing factors, correspond to different parameters in the simulations.

According to Calamosca et al., [2003], the critical angle is inherently dependent on entire detector analysis procedure, i.e. on the detector material choice, the chemical etching procedure as well as the detector analysis method at the optical microscope. Figure 7 also shows the simulated sensitivity for this chamber using 40° as critical angle and the same minimum energy as before. As can be seen, in this case a very good agreement with the experimental sensitivity obtained by Garawi [1996] was achieved. The results obtained by the developed Monte Carlo code gave good agreement with Mahlobo [1992] and Antovic et

al. [2007]. In general, detector sensitivities obtained by the main program are close to the experimental results.

3.2 Experimental results

Table 9 shows the experimental sensitivities related to each chamber according to equation (4). Due to the small values of sensitivities, it was assumed 80% of the radon concentration estimated by the NRPB monitor. We considered that the semipermeable membrane at the mouth of chambers was the responsible of that decrease.

Table 9. Experimental sensitivities for each chamber

Monitor code	Density rate (tracks.cm^{-2} .month^{-1})	Radon concentration (Bq/m^{3})	k Bq.month.m^{-3}/ (tracks.cm^{-2})	Sensitivity (1/k) (cm)
NRPB	**196,05**	**97,25**	**0,50**	**0,78**
F - b	129,39		0,60	0,64
A - b	155,70		0,50	0,77
E - a	810,15		0,10	4,02
N-b	75,83		1,03	0,38
I - a	90,23		0,86	0,45

Table 10. Monte Carlo simulations and experimental values

Monitor Code	E_{min} (MeV)	$\langle\theta_c\rangle$ (degrees)	f_1	Sexp (cm^{-1})	Scal (cm^{-1})	Min
F - b	0,2	40	0,2	1,24	1,23	3,05E-05
A - b	0,3	50	0	1,03	1,02	5,77E-05
N-b	0,1	45	0	0,60	0,64	1,39E-03
I - a	0,1	55	0	0,72	0,75	2,24E-03

By means of the developed M-C program, with these parameters we determine the calibration coefficient of PADC detector in a cylindrical diffusion chamber of any size, if chemical etching conditions and mode of track analysis are the same as the used for

calculations. The corresponding f_l fraction is taken according to the A/V ratio of the chamber. In other words, if another type of diffusion chamber is to be used, is not necessary to experimentally determine the calibration coefficient by their exposure to known radon concentration. Instead, simply enter their dimensions and the obtained values of E_{min} and $<\theta_{crit}$ in the developed Monte Carlo code. It is important to emphasize that the etched conditions and track analysis should remain unchanged.

Although the present experimental estimation of the critical angle is in good agreement with Fromm et al. [1988], the use of different etching conditions and acquisition apparatus resulted in a greater critical angle (15° difference) in comparison to the angle value reported by Dörschel et al. [2002]. In the results as reported by Eappen et al., [2002], the ^{212}Po was not considered.

4.- CONCLUSIONS

Based on the concept of effective volume and surface a computer program for calculating the PADC sensitivity for radon measurements with a diffusion chamber was developed. The M.C. Code was used to determine parameter values required for sensitivity calculations (E_{min}, θ_c, and f_1) related to different diffusion chambers. These parameters can be used for calibration of other designed chambers. The numerical examples and comparisons between experimental and calculated calibration coefficients show that the proposed method is applicable for uncertainties in order of 30%. These parameters were determined from a series of conducted experiments. The measured and modeled sensitivity values have been found to be in close agreement with each other considering a decrease in the inner chambers of 50%.

A program based on Monte Carlo simulations was developed to compute the partial and total sensitivities of PADC detector inside cylindrical and conical diffusion chambers for passive monitoring of radon in the environment. The validity of the implemented algorithm was proven by comparison of the calculated and experimentally reported sensitivities for diffusion chambers of different geometries and detectors with different areas.

The theoretical approach in this work can be used to design new dosimeters, especially for thoron, as currently used dosimeter devices exclude the ^{212}Po contributions. In general term, results of numerical examples and comparisons between experimental calibration coefficients with simulated one show that the proposed method is applicable for new monitors.

Acknowledgments

One of the co-Authors (L S-B) is grateful to the PUCP for the financial support granted as invited Visiting Professor. Detectors were supplied by TASL TRACK of Bristol UK authors are grateful for company support to the project. This research was founded by FINCyT (PIAP -3-P-671-14).

REFERENCES

Abo-Elmagd M & Soliman HA. (2009). *Measurement of the equilibrium factor between radon and its short-lived daughter products using CR-39 detector*. Isotope and Radiation Research **41**: 823-831.

Abu-Jarad F; Fremlin JH & Bull R. (1980). *A study of radon emitted from building materials using plastic a-track detectors*. Physics Medicine and Biology **25**: 683-694.

Antovic N; Vukotic P; Zekic R; Svrkota R & Ilic R. (2007). *Indoor radon concentrations in urban settlements on the Montenegrin Coast*. Radiation Measurements. **42**: 1573-1579.

Askari HR; Ghandi Kh; Rahimi M & Negarestani A. (2008). *Theoretical calculation on CR-39 response for radon measurements and optimum diffusion chambers dimensions.* Nuclear Instruments and Methods in Physics Research A **596**: 368–383.

Calamosca M; Penzo S & Gualdrini G. (2003). *Experimental determination of CR-39 counting efficiency to α particles to design the holder of a new radon gas dosimeter.* Radiation Measurements **36**: 217 – 219.

Dörschel B; Hermsdorf D & Reichelt U. (2002). *Experimental determination on the critical angle for particle registration and comparison with model predictions*. Radiation Measurements **35**: 189-193.

Durrani SA & Bull RK. *SOLID STATE NUCLEAR TRACK DETECTION*. Oxford, Pregamon Press. (1987).

Eappen KP & Mayya YS. (2004). *Calibration factors for LR-115 (type-II) based radon thoron discriminating dosimeter*. Radiation Measurements **38**: 5-17.

Fromm M; Chambaudet A & Membrey F. (1988). *Data bank for alpha particle tracks in CR39 with energies ranging from 0.5 to 5 MeV recording for various incident angles*. Nuclear Tracks and Radiation Measurements **15**: 115-118.

Garawi MS. (1996). *Measurement of radon concentration in private houses in the eastern part of Al-Qaseem province of Saudi Arabia*. Radiation Protection Dosimetry **63**: 227–230.

Howarth CB & Miles JCH. (2003). *Results of the 2002 NRPB Intercomparison of Passive Radon detectors. NRPB-W44.* National Radiological Protection Board, Chilton, Didcot, Oxon OX11 ORQQ.

Howarth CB. (2007). *Results of the 2004 Intercomparison of Passive Radon detectores. HPA-RPD-028.* Health Protection Agency. Centre of Radiation, Chemical and Environmental Hazards. Radiation Protection Division, Chilton, Didcot, Oxfordshire OX11 ORQ.

Howarth CB. (2009). *Results of the 2006 Health Protection Agency Intercomparison of Passive Radon detectores. HPA-RPD-053*. Health Protection Agency. Centre of Radiation, Chemical and Environmental Hazards. Radiation Protection Division, Chilton, Didcot, Oxfordshire OX11 ORQ.

Ismail AH & Jaafar MS. (2011). *Design and Construct Optimum Dosimeter to Detect Airborne Radon and Thoron Gas: Experimental*. Nuclear Instruments and Methods in Physics Research B **269**: 437-439.

Khayrat AH & Durrani SA. (1999). *Variation of alpha-particle track diameter in CR-39 as a function of residual energy and etching conditions*. Radiation Measurements **30**: 15-18.

Koo VSY; Yip CWY; Ho JPY; Nikezic D & Yu KN. (2002). *Experimental study of track density distribution on LR115 detector and deposition fraction of ^{218}Po in diffusion chamber*. Nuclear Instruments and Methods in Physics Research A **491**: 470.473.

Koo VSY; Yip CWY; Ho JPY; Nikezic D & Yu KN. (2003). *Deposition fractions of ^{218}Po in diffusion chambers*. Applied Radiation and Isotopes **59**: 49-52.

Mahlobo M & Farid SM. (1992). *Radon Dosimetry Using Plastic Nuclear Track Detector*. Medical Journal of Islamic World Academy of Sciences **5**: 153-157.

Mamont-Cieśla K; Stawarz O; Karpińska M; Kapała J; Kozak K; Grządziel D; Chałupnik S; Chmielewska I; Olszewski J; Przylibski TA & Żebrowski A. (2010). *Intercomparison of radon CR-39 detector systems conducted in CLOR's calibration chamber*. Nukleonica **55**: 589−593.

Mansy M; Sharaf MA; Eissa HM; El-Kamees SU & Abo-Elmag M. (2006). *Theoretical calculation of SSNTD response for radon measurements and optimum diffusion chambers dimensions*. Radiation Measurements **41**: 222-228.

McLaughlin JP & Fitzgerald B. (1994). *Models for determining the response of Passive alpha particle detectors to Radon and its progeny in cylindrical detecting volumes*. Radiation Protection Dosimetry **56**: 241-246.

Misdaq MA; Merzouki A; Elabboubi D & Sfairi T. (2001). *A new method for studying the transport of photons in various geological materials by combining the SSNTD technique with Monte Carlo simulations*. Radiation Measurements **33**:175-181.

Nikezic D; Yu KN & Stajic JM. (2014). *Computer program for the sensitivity calculation of a CR-39 detector in a diffusion chamber for radon measurements*. Review of Scientific Instruments 85: 022102.

Nikezic D & Yu KN. (2002). *Incidence characteristics of alpha particles on detectors irradiated in a radon + progeny atmosphere*. Nuclear Instruments and Methods in Physics Research B **187**: 492–498.

Palacios D & Sajo-Bohus L; Greaves E.D. (2005). *Radon progeny distributions inside a diffusion chamber and their contributions to track density in SSNT detectors*. Radiation Measurements **40**: 657-661.

Patiris DL & Ioannides KG. (2009). *Discriminative detection of deposited radon daughters on CR-39 track detectors using TRIAC II code*. Nuclear Instruments and Methods in Physics Research B **267**: 2440–2448.

Pressyanov D; Rusinov I & Simeonov G. (1999). *Radon progeny deposition in track-detection difusion Chambers.* Nuclear Instruments and Methods in Physics Research A **435**: 509-513.

Al-Nia'emi SHS. (2014). *Effects of Ultrasound in Etching and Detecting Parameters of CR-39 Detector*. Jordan Journal of Physics 7: 35-42.